

Possible interrelations among chemical freezeout conditions

A. Tawfik*

*Egyptian Center for Theoretical Physics (ECTP),
Modern University for Technology and Information (MTI), 11571 Cairo, Egypt and
World Laboratory for Cosmology And Particle Physics (WLCAPP), Cairo, Egypt*

M. Y. El-Bakry, D. M. Habashy, and M. T. Mohamed

Ain Shams University, Faculty of Education, Department of Physics, Rozi, Cairo, Egypt

E. Abbas

*World Laboratory for Cosmology And Particle Physics (WLCAPP), Cairo, Egypt and
Ain Shams University, Faculty of Education, Department of Physics, Rozi, Cairo, Egypt*

(Dated: March 1, 2022)

At thermal equilibrium, different chemical freezeout conditions have been proposed so far. They have an ultimate aim of proposing a universal description for the chemical freezeout parameters (T_{ch} and μ_b), which are to be extracted from the statistical fitting of different particle ratios measured at various collision energies with calculations from thermal models. A systematic comparison between these conditions is presented. The physical meaning of each of them and their sensitivity to the hadron mass cuts are discussed. Based on availability, some of them are compared with recent lattice calculations. We found that most of these conditions are thermodynamically equivalent, especially at small baryon chemical potential. We propose that further crucial consistency tests should be performed at low energies. The fireball thermodynamics is another way of guessing conditions describing the chemical freezeout parameters extracted from high-energy experiments. We endorse the possibility that the various chemical freezeout conditions should be interpreted as different aspects of one universal condition.

PACS numbers: 24.10.Pa, 12.38.Mh, 05.70.Ce

Keywords: Heavy-ion collisions, hadron resonance gas, chemical freezeout conditions, QCD phase diagram

I. INTRODUCTION

The high temperature and/or large energy density which are likely in relativistic collisions of nuclei are conjectured to derive the quantum-chromodynamic (QCD) matter, the hadrons, to deconfined quarks and gluons. The new phase of matter, the quark-gluon plasma (QGP), has been produced in the relativistic heavy-ion collider (RHIC) [1]. Reducing the QGP temperature disposes hadronization and the formed fireball is conjectured to go into chemical equilibrium, where the particle abundances are assumed to get fixed. Studying QGP and phase transition(s) at different collision energies belong to the main goals of the heavy-ions collisions experiments. This is partly possible through mapping out the QCD boundary separating hadrons from QGP phase. At very small baryon chemical potential (μ_b), the hadron-quark phase transition takes place as smooth cross-over [2], where the value of the pseudo-critical temperature reaches $\sim 155 \pm 9$ MeV for three quark flavors, for instance [3–7]. At large μ_b , the phase transition is of first order and can only be studied in QCD-like models [8–12].

The hadron resonance gas (HRG) model [8, 13, 14] is utilized by many authors in order to extract information about the chemical freezeout stage, in the final state. Confronting HRG calculations to the experimentally measured particle ratios or yields is implemented to find out the equilibrium chemical freezeout parameters (temperature T_{ch} and corresponding baryon chemical potential μ_b) assuring best fits. Various sets of these parameters are collected over the last 2 – 3 decades in the Large Hadron Collider (LHC), RHIC, the Super Proton Synchrotron (SPS), the Alternating Gradient Synchrotron (AGS) and the Schwerionen Synchrotron (SIS) facilities [15–18]. It was found that they follow regular patterns with the nucleus-nucleus center-of-mass energy ($\sqrt{s_{NN}}$). It was found that the baryon chemical potential (μ_b) and $\sqrt{s_{NN}}$ are indirect proportional

* <http://atawfik.net/>

to each other. At LHC, μ_b becomes very small indicating a nearly vanishing net-baryon density [8]. On the other hand, the freezeout temperature increases with increasing $\sqrt{s_{NN}}$. At high energies, T_{ch} reaches a limiting temperature, which apparently sets on at $\sqrt{s_{NN}} > 30$ GeV [15, 17]. Proposing a universal condition describing the dependence of T_{ch} on μ_b or on $\sqrt{s_{NN}}$ enters the literature under the name "*conditions for chemical freezeout*".

At equilibrium, the chemical freezeout boundary can be determined from different universal conditions [19–27]. A first condition was proposed in Ref. [19]. It assumes that T_{ch} and μ_b are characterized by a constant average energy per particle ~ 1 GeV [19]. Other phenomenological conditions have been proposed to give further explanations for the extracted T_{ch} and μ_b parameters at various energies. Their short list is chronically ordered as follows.

- Sum of the baryon and antibaryon densities $n_b + n_{\bar{b}} = 0.12 \text{ fm}^{-3}$ [20].
- Condition based on percolation theory [21].
- Normalized entropy density $s/T^3 \simeq 7$ [22, 23].
- Entropy per particle $s/n = 7.18$ [24–26].
- Trace anomaly $(\epsilon - 3p)/T^4 = 7/2$, where p is pressure and ϵ is energy density [27].
- $\kappa \sigma^2 = 0$ where σ^2 and κ are variance and kurtosis of conserved net charge respectively [28].
- Equal collision and expansion time [29].

Except for the last two conditions and the percolation theory, the remaining conditions shall be discussed in the present work.

It is obvious that the condition $s/T^3 = 7$ seems to coincide with $\epsilon/n = 1.08 \text{ GeV}$ [16]. Furthermore, at high $\sqrt{s_{NN}}$ (small μ_b), the dimensionless conditions s/n and s/T^3 are found almost equal, both approximative are 7. This observation raises the question if there are interrelations among the various chemical freezeout conditions? A comparison between three chemical freezeout conditions have been consider about ten years ago [16]. In the present, we extend it to include additional chemical freezeout conditions and to consider recent RHIC and LHC results. The main aspect of present work is finding out interrelations between some of the so-far proposed freezeout conditions.

In the present work, we study the equilibrium freezeout criteria and discuss their physical meanings. We also investigate their validity or ability in describing the recently deduced T_{ch} and μ_b results. Upon availability, some conditions are confronted to recent lattice QCD calculations [30]. The possible interrelations among different freezeout conditions are analysed, thermodynamically. It is found that many chemical freezeout conditions are thermodynamically equivalent, especially at small baryon chemical potential. The fireball thermodynamics is another way of guessing conditions against equations using T_{ch} and μ_b as extracted from particle ratios. To this end, the energy dependence of T_{ch} and μ_b shall be utilized in estimating the fireball thermodynamic properties at the chemical freezeout.

The present paper is organized as follows. Section II elaborates details about the hadron resonance gas (HRG) model. The different chemical freezeout conditions shall be discussed in section III. The possible interrelations among the various chemical freeze-out conditions shall be discussed in section IV. Section V shall be devoted to the properties of fireball thermodynamics at chemical freeze-out. the final conclusions and outlook shall be outlined in section VI.

II. HADRON RESONANCE GAS MODEL

In the HRG model [8, 13, 14], the formation of hadrons is controlled by the phase space and the conservation laws. For a large number of produced particles, the implementation of grand canonical ensemble (GCE) treatment is obviously justified. Assuming that the strong interactions are dominated by the dynamics leading to the resonance formation, these interactions are believed to be taken into consideration through including heavy resonances [31, 32]. In the hadronic phase, the grand canonical partition function is summed up over *single-particle partition functions* of stable hadron and unstable resonances

$$\ln Z(T, \mu, V) = \sum_i \pm \frac{V g_i}{2\pi^2} \int_0^\infty p^2 \ln \left\{ 1 \pm \lambda_i \exp \left[\frac{-\varepsilon_i(p)}{T} \right] \right\} dp, \quad (1)$$

where $\lambda_i = \exp(\mu_i/T)$ is the fugacity of i -th hadron, $\varepsilon_i(p) = (p^2 + m_i^2)^{1/2}$ is its dispersion relation, g_i is the degeneracy factor and \pm stands for fermions and bosons, respectively. The chemical potential related to i -th particle is given as $\mu_i = \mu_b B_i + \mu_s S_i + \mu_q Q_i$, where μ_s , μ_q , B_i , S_i and Q_i are strange, and charge chemical potential and baryon, strange and charge quantum number, respectively.

The thermodynamic properties of this QCD system can be obtained from the partition function, Eq. (1). In non-degenerate case, the pressure and number density of the i -th hadron or resonance can be written as

$$P_i(T, \mu_i) = \pm \frac{g_i T^2 m_i^2}{2\pi^2} \sum_{n=1}^{\infty} \frac{(\pm \lambda_i)^n}{n^2} K_2\left(\frac{nm_i}{T}\right), \quad (2)$$

$$n_i(T, \mu) = \pm \frac{g_i T m_i^2}{2\pi^2} \sum_{n=1}^{\infty} \frac{(\pm \lambda_i)^n}{n} K_2\left(\frac{nm_i}{T}\right). \quad (3)$$

where here \mp stands for fermions and bosons, respectively. The chemical potential and temperature are there to assure the conservation of strangeness, charge and baryon numbers. This can be fulfilled by bearing off the volume as $\sum_i n_i(T, \mu_i) S_i = 0$, $\sum_i n_i(T, \mu_i) Q_i / \sum_i n_i(T, \mu_i) B_i = Z/A$, where A and Z are the mass and atomic number of the colliding nuclei. So far, all expressions are quantum statistical. In discussing the results, the logarithm series is extracted, where the first term in Eqs. (2) and (3) stand for Maxwell-Boltzmann (MB) limit. We remark that the calculations of all quantities are performed through quantum statistical expressions.

It is worthwhile to highlight that the summation in the previous expressions includes contributions from light flavor hadrons. These are listed in the particle data group (PDG) [33] with zero-width approximation. Corrections due to repulsive interaction between hadrons at small distances (known as excluded-volume correction (EVC) [34]) is not taken into account, as it was concluded that these are practically irrelevant [27, 28]. Furthermore, the decay of unstable resonances is not taken into consideration.

In this regard, it intends to study the properties of the fireball at the stage of the chemical freezeout. It is worthwhile to mention that the calculations from the HRG model are performed at full chemical equilibrium, as it was evidenced that in most central high-energy collisions the system reaches full chemical equilibrium [35].

III. CHEMICAL FREEZEOUT CONDITIONS

It is conjectured that the quark-hadron phase transition occurs prior to the stage of chemical freezeout, which is defined as the state at which the inelastic interactions between produced hadrons cease as the mean free path becomes larger than the system size [36]. Consequently, the hadron yields are frozen, i.e. no further change in the particle number (chemistry is fixed) takes place. Fitting particle ratios (to maximally eliminate the volume effect) calculated to the thermal models to the experimentally measured ones results in the freezeout parameters, which are interpreted in terms of some universal conditions [19–27]. It is in order now to introduce their basic concepts and compare between their predications, especially in reproducing the recent experimental results on particle ratios and yields.

A. Average energy per particle

This criterion was proposed in Ref. [19] as a condition describing the dependence of T_{ch} on μ_b as extracted from SPS, AGS and SIS facilities. Later on, other parameters extracted at top SPS and RHIC energies match well with this condition [8, 13]. In a non-relativistic system, i.e. MB limit, the average energy per particle for i -th hadron or resonance reads [37],

$$\frac{\epsilon}{n} = \sum_i m_i \left[1 + \frac{3}{2} \frac{T}{m_i} + \frac{15}{8} \left(\frac{T}{m_i} \right)^2 + \dots \right]. \quad (4)$$

1. At low energies, it is conjectured that the system is dominated by nucleons. By using the nucleons mass ≈ 0.94 GeV, ϵ/n will have a little bit higher value [37].
2. At high energies, the system will be dominant by light mesons where ϵ/n can be considered as an average particle mass plus the temperature terms. Although the average mass of the particles in the system decreases, the temperature will increase [37].

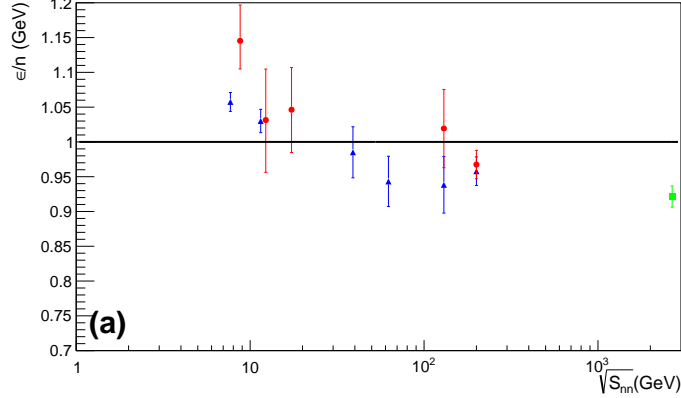


Fig. 1: The dependence of ϵ/n on energy at the freezeout parameters μ_b and T_{ch} [15, 17, 18] is depicted. The closed triangle symbols are results from Ref. [17], the circles stand for results from Ref. [15] and the square are the results at LHC energy [18]. The solid line represents $\epsilon/n = 1$ GeV as calculated from HRG model.

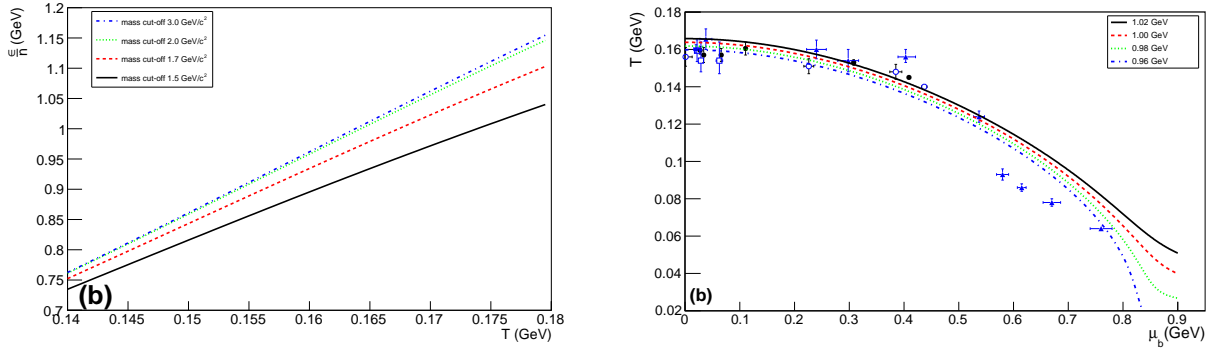


Fig. 2: Left-hand panel (b) shows the extracted parameters T_{ch} and μ_b at different values of ϵ/n . The closed diamond symbols are results from Ref. [15], the open circles stand for results from Ref. [41, 42], the open squares are the STAR results at 0 – 5% centrality [43] and the closed circles represent our results [17]. Right-hand panel (c) shows the dependence of ϵ/n on temperature at different resonance mass cut-off.

Joining all chemical freezeout parameters through $\epsilon/n \simeq 1$ GeV, seems to be a good guess for a universal freezeout condition [37].

It is worthwhile to recall that by assumed that the multi-hadron production is the QCD counterpart of the Hawking-Unruh radiation [38], it was predicted that the hadronic freezeout from the black-hole radiation for the average energy per hadron gives 1.09 GeV [39, 40]. This value amazingly agree with the thermal models. Thus, both approaches; namely thermal models and black hole radiation, not only confirm the idea of chemical freezeout condition but also approximately estimate the same value of averaged energy per particle at finite baryon chemical potential [40].

In order to determine the range of energies (or chemical potentials) in which this freeze-out condition $\epsilon/n = 1$ GeV (solid line) is valid, we compare with ϵ/n calculated from the extracted parameter using GCE and full chemical equilibrium [15, 17, 18] at different energies. The comparison is depicted in Fig. 1. The closed triangle symbols are results from Ref. [17], the circles show the results from Ref. [15] and the squares stand for results at LHC energy [18]. It is obvious that $\epsilon/n = 1$ GeV (solid line) lays above the phenomenologically deduced results, especially at the LHC energy. This is a natural consequence of determining T_{ch} at the ultra-relativistic high-energies 2.67 TeV, which is relatively less than the one observed at top RHIC energies. Concretely, in GCE and assuming full chemical equilibrium, ϵ/n is calculated by using the same parameters, T and μ_b , which have been presented in Refs. [15, 17, 18] at different energies.

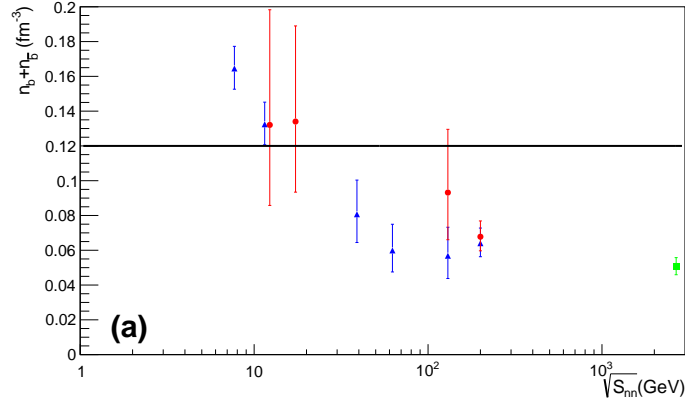


Fig. 3: The same as in Fig. 1 but here for $n_b + n_{\bar{b}}$. The solid line represents the constant value $n_b + n_{\bar{b}} = 0.12 \text{ fm}^{-3}$.

In left-hand panel of Fig.2 (b), the results on freezeout parameters calculated from HRG model under the condition of constant averaged energy per particle, are confronted to μ_b and T_{ch} , which are deduced from statistical fitting of various experimental particle ratios and corresponding calculations from HRG model, in which μ_b and T_{ch} are free parameters [15, 17, 41]. It is apparent that the most suitable values of ϵ/n are the ones less than 1 GeV whose limiting temperatures also agree well with the pseudo-critical temperature range predicted by the lattice QCD calculations [3, 4]. At high energies, a good agreement between this freezeout condition and the extracted parameters is found. The calculated values are a little bit higher than the phenomenologically deduced ones, especially at low energy. It should be stressed here that these calculations have been performed under GCE with zero-width which is not valid at AGS and SIS energies.

At vanishing baryon chemical potential, the right-hand panel Fig.2 (c) illustrates the dependence of ϵ/n on the freezeout temperature at various limits for mass cut-off, i.e. including/removing hadron resonances. It is obvious that the freezeout condition is obviously effected by the mass cut. With increasing the mass limits, the resonance contributions increase and consequently ϵ/n seems to increase as well. At different hadron resonance masses, different T_{ch} are able to fulfil the condition of constant ϵ/n . It has been assumed that EVC, in which a single hard-core is assumed for all hadrons and resonances in the MB limit has the same effect on both n and ϵ [16]. Both quantities shall be suppressed by almost the same factor [34].

B. Baryon and antibaryon particle density

The total baryon number density, $n_b + n_{\bar{b}}$, was proposed as a condition interpreting the extracted freezeout parameters [20]. Relative to the meaning of constant energy per particle, here another interpretation for the freeze-out parameters at different collision energies is proposed [20]. The correlations of baryons, such as baryon-baryon and baryon-meson interactions, are assumed to be the processes responsible for the chemical equilibrium [20]. The existing of such interactions weakens the applicability of this condition, as the chemical freeze-out is defined as a stage in which elastic scatterings become dominant, while this freezeout condition apparently relies on inelastic interactions, which likely drive the system towards chemical nonequilibrium.

In MB limit, the freezeout condition of the baryon density can be expressed as

$$n_b + n_{\bar{b}} = \sum_i \frac{g_i T m_i^2}{2 \pi^2} K_2 \left(\frac{m_i}{T} \right) \cosh \left(\frac{\mu_i}{T} \right), \quad (5)$$

where n_b is the baryon number density.

1. At very high energies, i.e. $\mu_i/T < 1$, the quantity $n_b + n_{\bar{b}}$ remains fixed. In this energy limit, T_{ch} remains constant, as well, while μ_b decreases with the energy.
2. At low energies, this criteria is effected by two factors; the increase in the hyperbolic function and the decrease in the other functions with increasing μ_i and decreasing temperature.

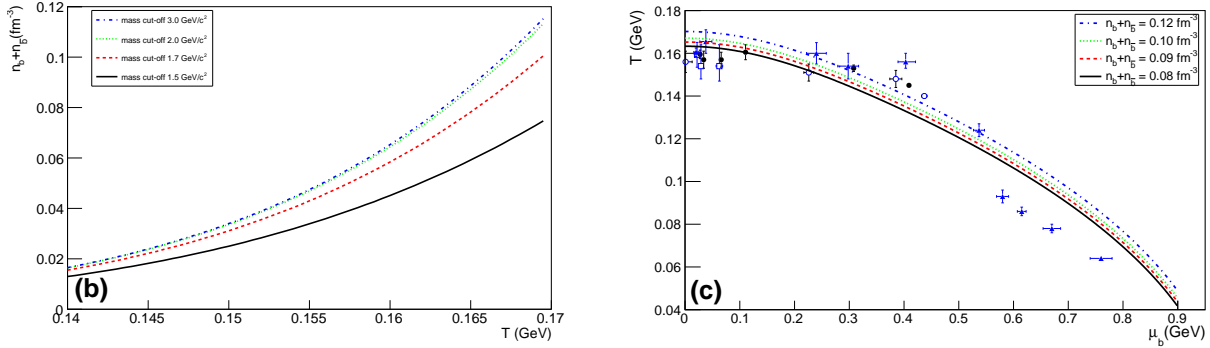


Fig. 4: Left-hand panel (b) shows the dependence of $n_b + n_{\bar{b}}$ on temperature at different resonance masses. Right-hand panel (c) presents different values for $n_b + n_{\bar{b}}$ and accordingly the extracted parameters T_{ch} and μ_b . The closed diamond symbols are results from Ref. [15], the open circles give the results from Ref [41], the open squares are STAR results at 0 – 5% centrality [43] and the closed circles represent our results [17].

3. In limit of $T \rightarrow 0$, the value of $n_b + n_{\bar{b}}$ will be nearly the nucleus baryon density.

We compare $n_b + n_{\bar{b}}$ with the calculations from GCE at full chemical equilibrium [15, 17, 18] and different energies. The comparison is depicted in Fig. 3. It is obvious that $n_b + n_{\bar{b}}$ increases at low energy. This could be due to appearance of baryons at mid-rapidity. At high energy, e.g. > 40 GeV, this freezeout condition takes a constant value because the change in μ_b/T becomes no longer significant.

This freeze-out condition is also effected by the hadron mass cuts. In Eq. 5, if the masses of included hadron resonances increase, the number of terms that shall be summed up to each others raises and consequently $n_b + n_{\bar{b}}$ increases. Also, we notice that the different values of T_{ch} are able to fulfil the condition at different masses of hadron resonances as shown in left-hand panel of Fig. 4 (b). It is obvious that $n_b + n_{\bar{b}}$ shall be suppressed when taking EVC into consideration [34]. Here, the suppression factor is not the same at all energies even when the hard-core radius is fixed. Thus, it is very essential to estimate the effects of EVC when implementing this freezeout condition. As mentioned earlier, EVC is not applied in the present calculations.

The right-hand panel of Fig. 4 (c) shows T_{ch} vs. μ_b at different values of $n_b + n_{\bar{b}}$ compared with the chemical freeze-out parameters T_{ch} and μ_b , which are extracted from the fits of measured particle ratios and the HRG calculations, in which T_{ch} and μ_b are taken as free parameters [15, 17, 41]. The parameters extracted at constant $n_b + n_{\bar{b}}$ show that at very high energies $n_b + n_{\bar{b}}$ should be reduced to 0.08 fm^{-3} . We notice that $n_b + n_{\bar{b}}$ increases with decreasing the energy (or increasing the chemical freezeout).

C. Normalized entropy density

It has been argued that the chemical freeze-out parameters can be described by a constant normalized entropy density (entropy density divided by T^3) [22, 23]. The quantity s/T^3 is assumed to measure the degrees of freedom (dof). The constant value refers to constant dof in the hadronic phase. During the phase transition the hadrons' dof should be replaced by the QGP's ones. Concretely, the value of s/T^3 was chosen at the pseudo-critical temperature as calculated in the lattice QCD simulations [44–47]. This assigned value is compatible with the quark flavors and masses used in the lattice calculations at vanishing baryon chemical potential. It was found that $s/T^3 = 5$ for two quark flavors and $s/T^3 = 7$ for three quark flavors [44–47]. Constant s/T^3 is conjectured to remain unchanged with increasing μ_b [22, 23]. Furthermore, the normalized entropy density was also used to separate a meson-dominant region from baryon-dominant one [49]. Accordingly, an explanation for the rapid variations of certain particle ratios that was observed at lower SPS energies [48] has been suggested [49]. It is obvious that when $T \rightarrow 0$, the thermal entropy density vanishes, as well.

In Fig. 5, s/T^3 calculated from the extracted parameter using GCE and full chemical equilibrium [15, 17, 18] is depicted at different energies. s/T^3 increases at low energy (AGS energies) because T^3 decreases much faster than s as the energy decreases. Thus, s/T^3 becomes no longer constant during chemical freeze-out at very large μ_b . s/T^3 value at LHC energy, equals the top RHIC energies values within the error.

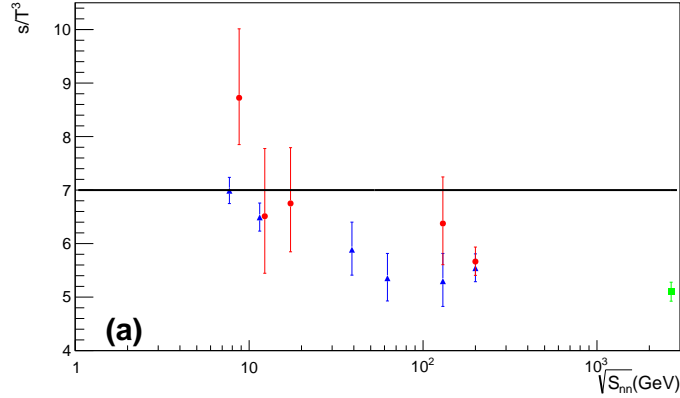


Fig. 5: The same as in Fig. 1 but here for constant s/T^3 . The solid line represents $s/T^3 = 7$.

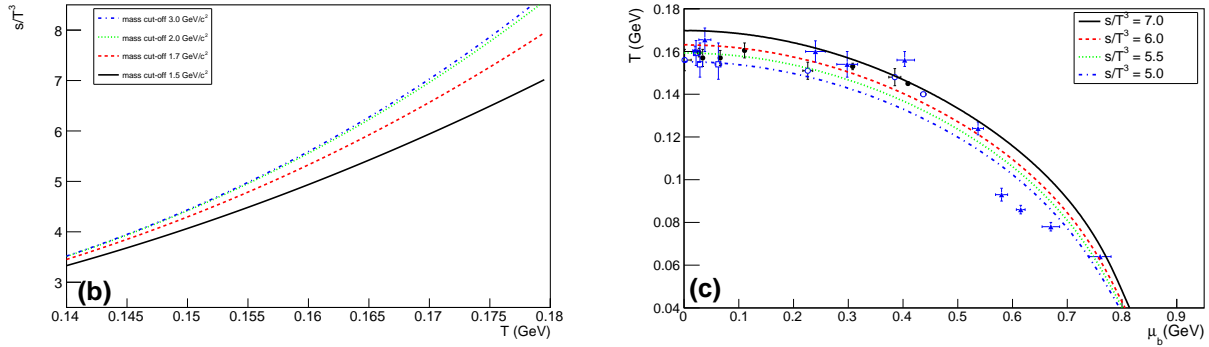


Fig. 6: Left-hand panel (b) gives the dependence of s/T^3 on the temperature at different resonance masses. Right-hand panel (c) shows different values of s/T^3 and the parameters T_{ch} and μ_b compared with the parameters deduced from the particle ratios. The closed diamond symbols are results from Ref. [15], the open circles stand for results from Ref. [41], the open squares are STAR results at 0 – 5% centrality [43] and the closed circles give our results [17].

The dof in the hadronic phase depend on the temperature, explicitly. This means that the hadronic dof should not remain fixed, at least from the thermodynamical point-of-view. Also, we highlight that EVC is conjectured to change the value of s/T^3 but its physical meaning remains unchanged. In other words, when EVC is implemented one may find another suitable guess for s/T^3 which will be less than the proposed values. Even this slightly smaller value does not change the ability of s/T^3 to reproduce the freeze-out parameters. At a certain temperature, adding more resonances by increasing the limits of the hadron resonance masses, s/T^3 increases as shown in left-hand panel of Fig. 6 (b). It is found that different values of T_{ch} are able to fulfil the condition of constant s/T^3 at different cuts in the resonance masses.

The right-hand panel of Fig. 6 (c) shows different values of s/T^3 and the corresponding parameters T_{ch} and μ_b calculated from HRG under the condition of constant s/T^3 compared with the ones deduced from fits of measured particle ratios and HRG calculations. We notice that lower values of s/T^3 are consistent with the deduced parameters as well as with the lattice QCD calculations. The best agreement is found if s/T^3 ranges between 4.70 and 6.0, this is corresponding to T_{ch} ranging from 150 and 160 MeV [30].

D. Entropy per particle

It was assumed that the entropy per particle can be utilized in describing the chemical freeze-out parameters [24–26]. The value of s/n was assumed as ~ 7 . The energy independence of s/n was interpreted as an

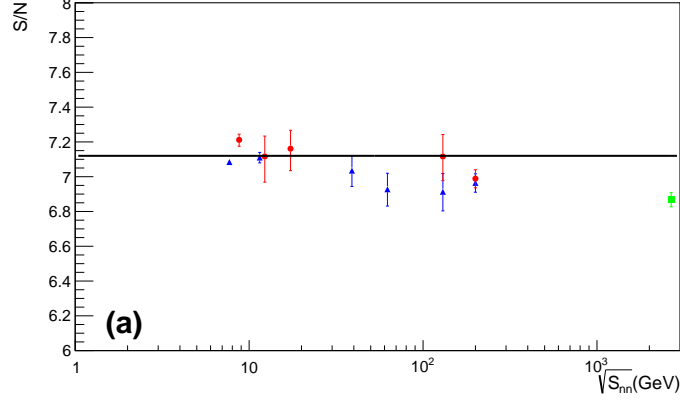


Fig. 7: The same as in Fig. 1 but here for constant s/n . The solid line represents $s/n = 7.18$ [25, 26].

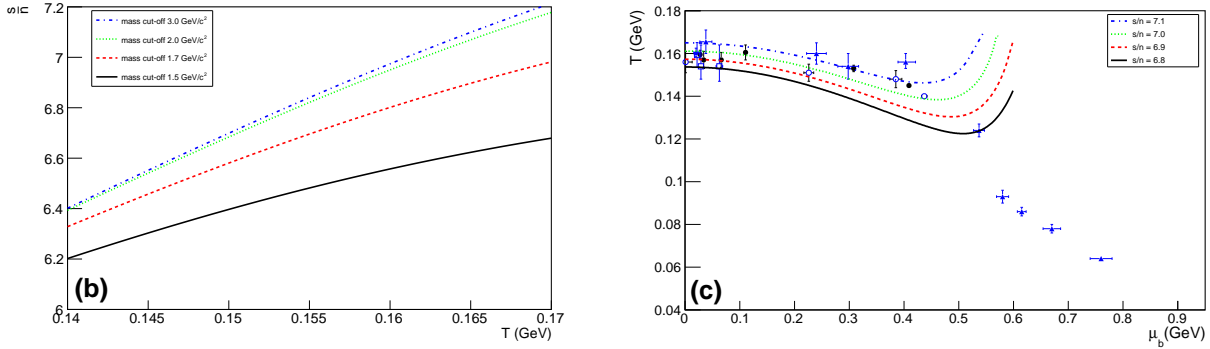


Fig. 8: Left-hand panel (b) shows the dependence of s/n on temperature at different resonance spectrum masses. Right-hand panel (c) depicts the freeze-out parameters T_{ch} and μ_b at different values of s/n and compares them with the ones from the particle ratios. The closed diamond symbols are results from Ref. [15], the open circles stand for the results from Ref. [41], the open squares are the STAR results at 0 – 5% centrality [43] and the closed circles give our results [17].

evidence for the adiabatic chemical hadron production in heavy-ion collisions [25, 26]. The entropy per particle is also assumed to measure the average of the available microstates, i.e. similar to the typical meaning of the entropy. Furthermore, s/n was used in framework of nonequilibrium statistical hadronization models in order to explain peaks in some particle ratios at low energy, such as K^+/π^+ [50].

Fig. 7 shows s/n calculated from the extracted parameter using GCE and full chemical equilibrium [15, 17, 18] at different energies. At high energies, $s/n \simeq 7$ shows a fair constant behaviour. However, $s/n \simeq 7$ requires a very high temperature in order to be satisfied at large baryon chemical potential $\mu_b > 0.5 \text{ GeV}$. The calculated value at LHC is a lower than the one calculated at RHIC energies. This might be interpreted from the observation that the extracted T_{ch} from the particle ratios at 2.67 TeV is less than the one at top RHIC energies.

This condition is apparently effected by the hadron mass cuts, especially at vanishing μ_b . A completely different values of T_{ch} can be observed at different cuts of the resonance masses, right-hand panel of Fig. 8 (b). This also illustrates how s/n is sensitive to the hadron mass cuts and shows that different T_{ch} can be obtained at different values of s/n . If both quantities n and s are suppressed by the same factor, for instance, by assuming a single hard-core for all hadrons in MB limit [34], it seems safe to study s/n with or without EVC.

The right-hand panel of Fig. 8 (c) depicts the freeze-out parameters T_{ch} and μ_b deduced at different values of s/n and compared with the recently extracted parameters from fits of experimental particle ratios and their calculations from HRG model. The agreement between the predicted values of s/n and extracted parameters is limited at small μ_b . This suggests a limiting value of s/n around 7 at high temperature but when the temperature decreases the extracted parameters likely suggest smaller values, as s/n diverges at large μ_b [26].

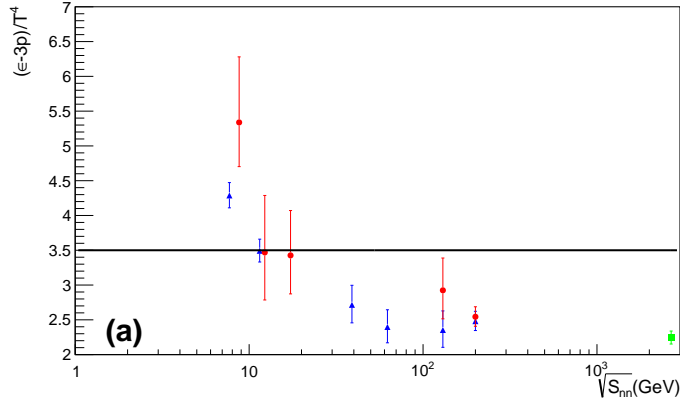


Fig. 9: The dependence of s/n on energy calculated at the freezeout parameters μ_b and T_{ch} [15, 17, 18] is given. The closed triangle symbols are results from Ref. [17], the circles stand for results from Ref. [15] and the square is the results at LHC energy [18]. The solid line represents the constant value $(\epsilon - 3p)/T^4 = 3.5$ [27].

This can be understood as a decrease in the average possible microstates with increasing temperature, which obviously contradicts the second law of thermodynamics.

E. Trace Anomaly

The QCD trace anomaly $(\epsilon - 3p)/T^4$ (also known as interaction measure) is finite in the hadron phase and vanishes in the QGP phase. According to lattice QCD simulations, the trace anomaly shows a peak near the pseudo-critical temperature indicating the phase transition and the appearance of massive quasiparticles [51]. This quantity was used as a novel chemical freeze-out condition [27] reproducing a universal description for T_{ch} and μ_b . The value assigned to it is deduced from the lattice QCD calculations. It is worthwhile to highlight that the lattice QCD calculations [52] show a shift in the trace anomaly curve towards lower T at large μ_b [52]. This means that the resulting T_{ch} would be decreasing with increasing μ_b .

Fig. 9 depicts $(\epsilon - 3p)/T^4$ calculated from the extracted freezeout parameters at different energies by using GCE and full chemical equilibrium [15, 17, 18]. At low energy, it is obvious that $(\epsilon - 3p)/T^4$ increases. At high energy (> 40 GeV), this condition takes a constant value. Thus, the ratio $(\epsilon - 3p)/T^4$ becomes no longer constant during chemical freeze-out at very large μ_b .

In BM limit, the trace anomaly can be written as

$$\frac{\epsilon - 3p}{T^4} = \sum_i g_i \left(\frac{m_i}{T}\right)^3 K_1\left(\frac{m_i}{T}\right) \exp\left(\frac{\mu_i}{T}\right). \quad (6)$$

In Eq. (6), when the mass cut is increased the terms that will be summed increase and the quantity $(\epsilon - 3p)/T^4$ increases too. At different masses, different values of T_{ch} are able to fulfil conditions of constant trace anomaly, left-hand panel of Fig. 10 (b). The EVC changes the value of $(\epsilon - 3p)/T^4$ but not the idea that represents. In other words, when ECV is implemented one might find another guess for $(\epsilon - 3p)/T^4$.

From recent lattice QCD calculations [30], $(\epsilon - 3p)/T^4$ can be determined between 2.09 and 2.76. This is corresponding to temperature ranging between 150 and 160 MeV. As the temperature decreases, higher values of $(\epsilon - 3p)/T^4$ are needed. This is illustrated in right-hand panel of As Fig. 10 (c).

IV. INTERRELATIONS AMONG CHEMICAL FREEZE-OUT CONDITIONS

We found that at small baryon chemical potential, the conditions $s/T^3 = 7$ seems to coincide with $\epsilon/n = 1.08$ GeV [16]. Both conditions have been interpreted by Hawking-Unruh mechanism [38] for the particle production in high-energy collisions. Almost identical values, $s/T^3 = 7.4$ and $\epsilon/n = 1.09$ GeV have been

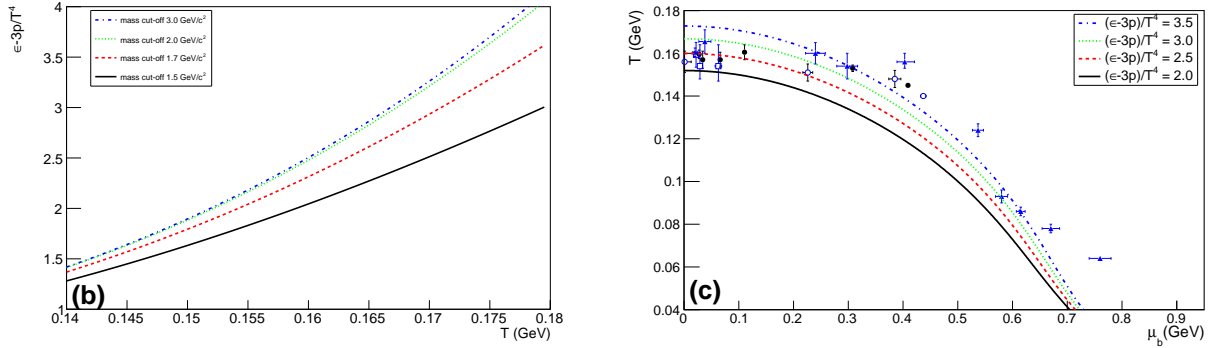


Fig. 10: Left-hand panel (b) shows the dependence of $(\epsilon - 3p)/T^4$ on temperature at different resonance masses. Right-hand panel (c) gives freeze-out parameters T_{ch} and μ_b determined as different $(\epsilon - 3p)/T^4$ and compared with the ones deduced from particle ratios. The closed diamond symbols are results from Ref. [15], the open circles stand for results from Ref. [41], the open squares represent the STAR results at 0 – 5% centrality [43] and the closed circles are our results [17].

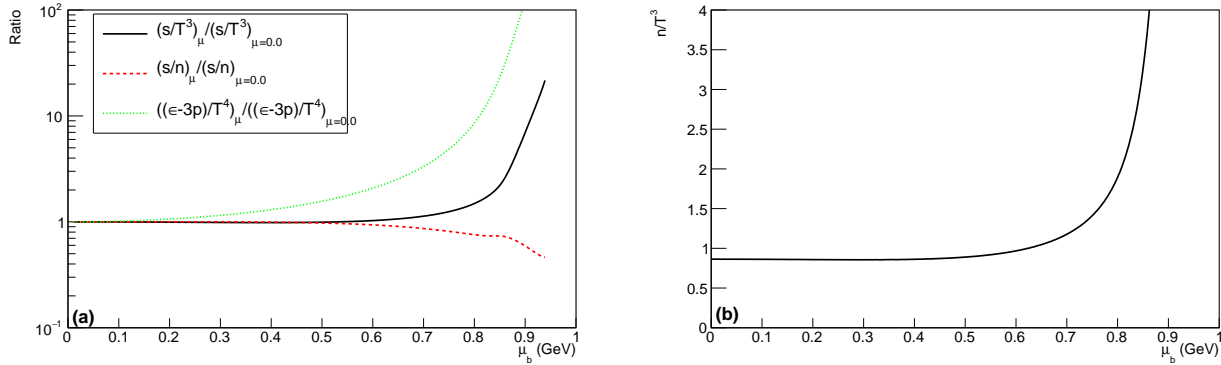


Fig. 11: Left-hand panel (a) shows the stability of s/T^3 , s/n and $(\epsilon - 3p)/T^4$ normalized to the same quantity but at $\mu_b = 0$ is given as a function of μ_b . Right-hand panel (b) depicts the dependence of n/T^3 on μ_b .

determined [39, 40]. Furthermore, at high energies, the freeze-out conditions s/n and s/T^3 both have almost the same value. This leads to a kind of interconnection between these different chemical conditions.

1. It is obvious ϵ/n and s/n can be related to each other

$$\sum_i \epsilon_i = T \sum_i s_i + \sum_i \mu_i n_i - \sum_i p_i, \quad (7)$$

$$\frac{\epsilon}{n} = T \left(\frac{s}{n} - 1 \right) + \frac{\sum_i \mu_i n_i}{\sum_i n_i}, \quad (8)$$

using $\sum_i p_i / \sum_i n_i = T$ in MB approximation.

At small baryon chemical potential, let us assume $T = 0.16$ GeV, for instance, then from the condition $\epsilon/n = 1$ GeV, we get $s/n = 7.25$. This means that both conditions are thermodynamically equivalent. But with increasing μ_b , s/n becomes no longer constant even at constant ϵ/n . The dependence of s/n at finite μ_b normalized to the corresponding value at vanishing μ_b at a fixed ϵ/n is depicted in left-hand panel of Fig. 11 (a). When μ_b increases, n/T^3 does remain constant, [right-hand panel of Eq. 8 (b)]. Accordingly, the temperature varies. This leads to a departure in the value of the freezeout conditions with respect to their values at vanishing μ_b at constant ϵ/n . In other words, both conditions can not be

achieved, simultaneously. Although, there is a small deviation in s/n , which can be interpreted due to the huge change in T_{ch} as predicted by s/n condition at a certain μ_b [right-hand panel of Fig. 8 (c)].

2. In MB limit, the pion number density is given as

$$n_\pi = \frac{g_\pi}{2\pi^2} T m_\pi^2 K_2\left(\frac{m_\pi}{T}\right) \exp\left(\frac{\mu_\pi}{T}\right). \quad (9)$$

In non-relativistic limit, i.e. $m_\pi \ll T$ and when ignoring the chemical potential and assuming that $K_2(m_\pi/T)$ can be approximated as $2T^2/m_\pi^2$, then

$$n_\pi \approx \frac{3}{\pi^2} T^3. \quad (10)$$

At high energy, the pions become dominating the formed fireball. Assuming that n/T^3 remains constant in high-energy collisions, then it is expected that s/T^3 turns to be related to s/n as long as n/T^3 remains constant. The value of n/T^3 is approximated to 0.86 at $\epsilon/n = 1$ GeV as shown in right-hand panel of Fig. 11 (b). At small baryon chemical potential, both conditions (s/n and s/T^3) are equivalent. At large baryon chemical potential, this equivalence seems to be destroyed. Thus, s/n , s/T^3 and ϵ/n become constants at small chemical potential.

3. In MB limit, s/T^3 and $(\epsilon - 3p)/T^4$ can be related to each other,

$$\frac{s}{T^3} = \frac{1}{T^4} \sum_i (p_i + \epsilon_i - T \mu_i n_i), \quad (11)$$

$$\frac{\epsilon - 3p}{T^4} = \frac{\sum_i s_i}{T^3} - \frac{4}{T^3} \sum_i n_i (1 - 0.25\mu_i). \quad (12)$$

As discussed earlier, at small baryon chemical potential, n/T^3 is approximately constant. This leads to $\sum_i (\epsilon_i - 3p_i)/T^4 \approx 3.56$.

The summary of three interrelations is illustrated in Fig. 11. At small baryon chemical potential, s/T^3 , s/n , $(\epsilon - 3p)/T^4$ and n/T^3 are approximately constant at constant ϵ/n . This conclusion does not contradict the results depicted in Figs. 1, 3, 5, 7 and 9, as the constancy in s/T^3 , s/n , and $(\epsilon - 3p)/T^4$ is based in their normalization to their corresponding value at $\mu = 0$. But, as the baryon chemical potential increases, these freeze-out conditions become energy-dependent. In high-energy collisions, the thermodynamic quantities are weakly effected by the chemical potentials and thus remain approximately constant as well as the ratios between each pair of them.

V. PROPERTIES OF FIREBALL THERMODYNAMICS AT CHEMICAL FREEZE-OUT

It is assumed that the chemically equilibrated hadron gas emerges from the fireball produced in the high-energy collision. Determining its thermodynamic properties such as temperature, energy density, entropy etc. represents a great challenge to be related to the measurable properties in the final state, such as rapidity, momentum and the hadron multiplicity. As discussed in earlier sections, the hadron multiplicities and their ratios can be explained in terms of chemical freeze-out parameters, T_{ch} and μ_b , of the fireball. In the present work, it intends to redefine certain uniform conditions, e.g. chemical freeze-out conditions, which should be also satisfied by the thermodynamic properties of the fireball at the stage of the chemical freeze-out. In section III, we have compared the extracted T_{ch} and μ_b from the measured particle ratios with the parameters obtained from different freeze-out conditions. We try to highlight some details about the physical properties of the fireball. The ultimate goal is the characterization of the dynamics of the fireball expansion and how this can be accessed by the given chemical freeze-out conditions.

Here, we propose another way to check the chemical freeze-out conditions. We show that their values can be obtained from the extracted freeze-out parameters T_{ch} and μ_b [17], which in this case represent the thermodynamic properties of the fireball at full chemical equilibrium and in most central collisions at mid-rapidity. From T_{ch} and μ_b [17], we find for instance that the resulting temperature agrees well with the lattice QCD pseudo-critical temperature.

Furthermore, from the HRG model at $\mu_b \leq 0.4$ GeV, following thermodynamic quantities can be determined

- pressure (p) lies between 0.057 and 0.065 GeV/fm⁻³,
- energy density (ϵ) ranges between 0.393 and 0.4312 GeV/fm⁻³, and
- entropy density (s) extends between 2.68 and 3.08 fm⁻³,

and accordingly the freeze-out conditions lead to

- energy per particle (ϵ/n) lies between 0.95 and 1.05 GeV,
- entropy per particle (s/n) ranges between 6.94 and 7.07,
- normalized entropy density (s/T^3) extends between 5.4 and 6.8, and
- trace anomaly $[(\epsilon - 3p)/T^4]$ takes a value within 2.5 and 4.

It is obvious that these values which are estimated for the chemical freeze-out conditions agree well with the values which are assigned to them, phenomenologically. Furthermore, small changes in the thermodynamic properties are noticed at $\mu_b \leq 0.4$ GeV. In this μ_b -range, the temperature does not vary so much. Additionally, we conclude that the real test of the chemical freeze-out conditions at low energy (large μ_b) is the one where T_{ch} and μ_b are changing very rapidly with changing $\sqrt{s_{NN}}$. In this energy (or μ_b) range, the differentiation between the various chemical freeze-out conditions likely becomes obvious.

VI. CONCLUSIONS AND OUTLOOK

We have reanalysed some chemical freeze-out conditions in framework of HRG model and compared them with new ones. The calculations are performed in full chemical equilibrium in grand canonical ensemble with zero-width approximation. The excluded-volume corrections are not applied.

Most of conditions match well with the chemical freeze-out parameters, which are extracted from fitting the measured particle ratios with their calculations in the HRG model. In doing this, at least two free parameters, T_{ch} and μ_b are to be tuned. This assures the conservation laws of strangeness, charge and baryon numbers and are to be controlled by the phase space.

Some of these conditions are ratios between two extensive thermodynamic quantities, such as s/n and ϵ/n . Thus, it is almost identical to study them with or without excluded-volume corrections. But, others are effected by the excluded-volume corrections, such as s/T^3 , $(\epsilon - 3p)/T^4$ and $n_b + n_{\bar{b}}$. Here we assume that the radii of mesons and baryons are vanishing. The scope of this work is defining interrelations among various chemical freeze-out conditions. EVC probably comes up with corrections to various thermodynamic quantities. These likely should not change their interrelations.

It is obvious that all conditions are effected by the mass cut-off, especially at small μ_b , as given in the left-had panels of the first five figures. With increasing the resonance masses, their contributions increase and consequently lower temperatures are able to fulfil the given freeze-out conditions. Thus, at different resonance mass limits, different T_{ch} are able to fulfil the condition.

Regarding the interrelations among the various chemical freeze-out conditions, we find that

1. the condition $s/T^3 = 7$ coincides with $\epsilon/n = 1.08$ GeV [16], especially at small baryon chemical potential.
2. At small μ_b , the two conditions s/n and s/T^3 have approximately the same dimensionless value, i.e. 7. It can be assume that these interrelations can be generalized to the whole range of chemical potentials.
3. This would make it possible to consider the possibility to interpret the different conditions as different aspects of one universal condition. At small or even vanishing μ_b , $\epsilon/n = 1$ GeV. This value leads to $s/n = 7.25$.
4. s/T^3 turns to be related to s/n as long as n/T^3 remains constant.
5. At small baryon chemical potential, a clear relation is found between trace anomaly, normalized entropy and n/T^3 . As long as n/T^3 remains constant and μ_b is very small, $(\epsilon - 3p)/T^4 \approx 3.56$ and $s/T^3 = 7$ are found equivalent.

Most of freeze-out conditions coincide with the experimental measurements at high energy. This agreement becomes weaker, at lower energies. We would like to highlight that these conclusions should be restricted to the constraints made in this study; full chemical equilibrium, zero-width approximation and grand-canonical ensemble framework. But these conclusions are correct at high energy. At lower energies, the freeze-out conditions are no longer dominant or precise in order to draw edge-cutting conclusion. The proposed interrelations among the various chemical freeze-out conditions, which have been so far achieved partly, lead to interpreting the different conditions as different aspects from fewer universal conditions..

Recent studies suggest that the chemical freeze-out occurs in a slightly non-equilibrium situation, for instance, due to hadron inelastic rescattering and non-equilibrium quark occupation factors (γ_q and γ_s). The latter is widely criticized due to the additional free parameters included in the statistical fits [53]. The early one was also critically commented because of the absence of stringent test, especially with yields of light nuclei, in which no additional free parameter is available [18]. The light nuclei are sensitive to the increasing in the powers of the quark chemical potentials. For sake of completeness, we highlight that the production of hypertritons, for instance, is in good agreement with the standard statistical hadronization picture. But they are largely overpredicted (by a factor of 6), at non-equilibrium γ_q and γ_s .

-
- [1] K. Gyulassy and L. McLerran, "New forms of QCD matter discovered at RHIC", Nucl. Phys. A **750**, 30 (2005).
 - [2] Y. Aoki, G. Endrodi, Z. Fodor, S.D. Katz and K.K. Szabo, "The order of the quantum chromodynamics transition predicted by the standard model of particle physics", Nature **443**, 675 (2006).
 - [3] A. Bazavov *et al.*, "Chiral and deconfinement aspects of the QCD transition", Phys. Rev. D **85**, 054503 (2012).
 - [4] T. Bhattacharya *et al.*, (HotQCD Collaboration), "The QCD phase transition with physical-mass, chiral quarks", Phys. Rev. Lett. **113**, 082001 (2014).
 - [5] C. R. Allton, S. Ejiri, S. J. Hands, O. Kaczmarek, F. Karsch, E. Laermann, Ch. Schmidt and L. Scorzato, "QCD thermal phase transition in the presence of a small chemical potential", Phys. Rev. D **66**, 074507 (2002).
 - [6] K. Fukushima, "Chiral effective model with the Polyakov loop", Phys. Lett. B **591**, 277 (2004).
 - [7] B. J. Schaefer, J. M. Pawłowski and J. Wambach, "Phase structure of the Polyakov-quark-meson model", Phys. Rev. D **76**, 074023 (2007).
 - [8] Abdel Nasser Tawfik, "Equilibrium statistical-thermal models in high-energy physics", Int. J. Mod. Phys. A **29**, 1430021 (2014).
 - [9] A. Tawfik, N. Magdy and A. Diab, "Polyakov linear SU(3) σ model: Features of higher-order moments in a dense and thermal hadronic medium" Phys. Rev. C **89**, 055210 (2014).
 - [10] Abdel Nasser Tawfik and Abdel Magied Diab, "Polyakov SU(3) extended linear- model: Sixteen mesonic states in chiral phase structure", Phys. Rev. C **91**, 015204 (2015).
 - [11] Nada Ezzelarab, Abdel Magied Diab and Abdel Nasser Tawfik, "Equation of State in Non-Zero Magnetic Field", J. Phys. Conf. Ser. **668**, 012102 (2016).
 - [12] Abdel Nasser Tawfik, "Transport coefficients and quark-hadron phase transition(s) from PLSM in vanishing and finite magnetic field", J. Phys. Conf. Ser. **668**, 012082 (2016).
 - [13] P. Braun-Munzinger, K. Redlich and J. Stachel, "Particle Production in Heavy Ion Collisions", In *Hwa, R.C. (ed.) *et al.: Quark gluon plasma** 491-599; nucl-th/0304013.
 - [14] F. Becattini, "An introduction to the Statistical Hadronization Model", 0901.3643 [hep-ph].
 - [15] A. Andronic, P. Braun-Munzinger and J. Stachel, "Hadron production in central nucleus-nucleus collisions at chemical freeze-out", Nucl. Phys. A **772**, 167 (2006).
 - [16] J. Cleymans, H. Oeschler, K. Redlich and S. Wheaton, "Comparison of Chemical Freeze-Out Criteria in Heavy-Ion Collisions", Phys. Rev. C **73**, 034905 (2006).
 - [17] A. Tawfik and E. Abbas, "Thermal Description of Particle Production in Au-Au Collisions at STAR Energies", Phys. Part. Nucl. Lett. **12**, 521 (2015).
 - [18] J. Stachel, A. Andronic, P. Braun-Munzinger and K. Redlich, "Confronting LHC data with the statistical hadronization model", J. Phys. Conf. Ser. **509**, 012019 (2014).
 - [19] J. Cleymans and K. Redlich, "Unified Description of Freeze-Out Parameters in Relativistic Heavy Ion Collisions", Phys. Rev. Lett. **81**, 5284 (1998).
 - [20] P. Braun-Munzinger and J. Stachel, "Particle ratios, equilibration and the QCD phase boundary", J. Phys. G: Nucl. Part. Phys. **28**, 1971 (2002).
 - [21] V. Magas and H. Satz, "Conditions for confinement and freeze-out", Eur. Phys. J. C **32**, 115 (2003).
 - [22] A. Tawfik, "Condition driving chemical freeze-out", Euro. phys. Lett., **75**, 420 (2006).
 - [23] A. Tawfik, "A universal description for the freeze-out parameters in heavy-ion collisions", Nucl. Phys. A **764**, 387 (2006).
 - [24] S. K. Tiwari, P. K. Srivastava and C. P. Singh, "Description of hot and dense hadron-gas properties in a new

- excluded-volume model*" *Phys. Rev. C* **85**, 014908 (2012).
- [25] D.R. Oliinychenko, K.A. Bugaev and A.S. Sorin, "Investigation of hadron multiplicities and hadron yield ratios in heavy ion collisions", *Ukr. J. Phys.* **58**, 211 (2013).
 - [26] A. Tawfik, H. Magdy and E. Gamal, "Comment on Investigation of Hadron Multiplicity and Hadron Yield Ratios in Heavy-Ion Collisions", *Ukr. J. Phys.* **58**, 933 (2013).
 - [27] A. Tawfik "Constant Trace Anomaly as a Universal Condition for the Chemical Freeze-Out", *Phys. Rev. C* **88**, 035203 (2013).
 - [28] A. Tawfik, "Chemical Freeze-Out and Higher Order Multiplicity Moments", *Nucl. Phys. A* **922**, 225 (2014).
 - [29] D. B. Blaschke, J. Berdermann, J. Cleymans and K. Redlich, "Chiral condensate and chemical freeze-out", *Phys. Part. Nucl. Lett.* **8**, 811 (2011).
 - [30] A. Bazavov *et al.*, "The equation of state in (2+1)-flavor QCD", *Phys. Rev. D* **90**, 094503 (2014).
 - [31] E. Beth and G.E. Uhlenbeck, "The quantum theory of the non-ideal gas. II. Behavior at low temperatures", *Physica* **4**, 915 (1937).
 - [32] R. Dashen, S.-K. Ma and H.J. Bernstein: "S Matrix formulation of statistical mechanics", *Phys. Rev.* **187**, 345 (1969).
 - [33] J. Beringer *et al.* [Particle Data Group], "Review of Particle Physics", *Phys. Rev. D* **86**, 010001 (2012).
 - [34] V.V. Begun, M. Gazdzicki and M.I. Gorenstein, "Hadron-Resonance Gas at Freeze-out: Reminder on Importance of Repulsive Interactions", *Phys. Rev. C* **88**, 024902 (2013).
 - [35] Abdel Nasser Tawfik, M.Y. El-Bakry, D.M. Habashy, M.T. Mohamed and Ehab Abbas, "Degree of Chemical Non-equilibrium in Central Au-Au Collisions at RHIC energies", *Int. J. Mod. Phys. E* **24**, 1550067 (2015).
 - [36] J. Cleymans, K. Redlich, H. Satz and E. Suhonen, "The hadronisation of a quark-gluon plasma", *Z. Phys. C* **58**, 347 (1993).
 - [37] J. Cleymans and K. Redlich, "Chemical and thermal freeze-out parameters from 1A to 200A GeV", *Phys. Rev. C* **60**, 054908 (1999).
 - [38] P. Castorina, D. Kharzeev and H. Satz, "Thermal Hadronization and Hawking-Unruh Radiation in QCD", *Eur. Phys. J. C* **52**, 187 (2007).
 - [39] P. Castorina, A. Iorio and H. Satz, "Hadron Freeze-Out and Unruh Radiation", *Int. J. Mod. Phys. E* **24**, 1550056 (2015).
 - [40] Abdel Nasser Tawfik, Hayam Yassin, and Eman R. Abo Elyazeed, "Chemical Freeze-Out in Hawking-Unruh Radiation and Quark-Hadron Transition", *Phys. Rev. D* **92**, 085002 (2015).
 - [41] F. Becattini, M. Bleicher, T. Kollegger, T. Schuster, J. Steinheimer and R. Stock "Hadron Formation in Relativistic Nuclear Collisions and the QCD Phase Diagram", *Phys. Rev. Lett.* **111**, 082302 (2013).
 - [42] R. Stock, F. Becattini, M. Bleicher, T. Kollegger, T. Schuster and J. Steinheimer "Hadronic Freeze-Out in A+A Collisions meets the Lattice QCD Parton-Hadron Transition Line", *PoS CPOD* **2013**, 011 (2013).
 - [43] B. I. Abelev *et al.* [STAR Collaboration], "Systematic Measurements of Identified Particle Spectra in pp, d+Au and Au+Au Collisions from STAR", *Phys. Rev. C* **79**, 034909 (2009).
 - [44] F. Karsch, K. Redlich and A. Tawfik, "Hadron Resonance Mass Spectrum and Lattice QCD Thermodynamics", *Eur. Phys. J. C* **29**, 549 (2003).
 - [45] F. Karsch, K. Redlich and A. Tawfik, "Thermodynamics at Non-Zero Baryon Number Density: A Comparison of Lattice and Hadron Resonance Gas Model Calculations", *Phys. Lett. B* **571**, 67 (2003).
 - [46] K. Redlich, F. Karsch and A. Tawfik, "Heavy-ion collisions and lattice QCD at finite baryon density", *J. Phys. G* **30**, S1271 (2004).
 - [47] A. Tawfik, "QCD phase diagram: A comparison of lattice and hadron resonance gas model calculations", *Phys. Rev. D* **71**, 054502 (2005).
 - [48] M. Gazdzicki *et al.* [NA49 Collaboration], "Report from NA49", *J. Phys. G* **30**, S701 (2004).
 - [49] J. Cleymans, H. Oeschler, K. Redlich and S. Wheaton, "Transition from baryonic to mesonic freeze-out", *Phys. Lett. B* **615**, 50 (2005).
 - [50] A. Tawfik, "Particle Ratios in Heavy-Ion Collisions", *Fizika B* **18**, 141 (2009).
 - [51] A. Bazavov *et al.*, "On trace anomaly in 2+1 flavor QCD", *PoS LATTICE* **2012**, 069 (2012).
 - [52] Sz. Borsnyi, G. Endr di, Z. Fodor, S. D. Katz, S. Krieg, C. Ratti, and K. K. Szabo, "QCD equation of state at nonzero chemical potential: continuum results with physical quark masses at order μ^2 ", *JHEP* **1208**, 053 (2012).
 - [53] Michele Floris, "Hadron yields and the phase diagram of strongly interacting matter", *Nucl. Phys. A* **931**, 103 (2014).